Journal of Electronics, Electromedical Engineering, and Medical Informatics
Multidisciplinary: Rapid Review: Open Access Journal **Vol. 6, No. 1, January 2024, pp: 23-31; eISSN: 2656-8632**

RESEARCH ARTICLE **OPEN ACCESS**

Manuscript received November 1, 2023; revised December 30, 2023; accepted December 30, 2023; date of publication January 20, 2024
Digital Object Identifier (**DOI**): https://doi.org/10.35882/jeemi.v6i1.339

How to cite: Masato Sawatari, and Shunko A. Inada, Development and Evaluation of Biochips Specialized for Cell Counting, Journal of Electronics, Electromedical Engineering, and Medical Informatics, vol. 6, no. 1, pp. 23-31, January 2024.

Development and Evaluation of Biochips Specialized for Cell Counting

Masato Sawatari[1], and Shunko A. Inada[2]
[1] Department of Computer Science and Electrical Engineering, Graduate School of Science and Technology, Kumamoto University, Kumamoto, Japan.
[2] Division of Biomedical Engineering, Faculty of Advanced Science and Technology, Kumamoto University, Kumamoto, Japan.

Corresponding author: Shunko A. Inada (e-mail: inada@cs.kumamoto-u.ac.jp).

ABSTRACT Cell counters, which are dedicated cell analyzers, can be used to analyze cellular status. Cell counters are smaller and less expensive (about $13,000) than other cell analysis devices such as flow cytometers (FACS), real-time PCR, and sequencers, and can discriminate between life and death of fluorescently stained cells. Cell death can be roughly divided into two types: apoptosis and necrosis, but Cell counters cannot distinguish between apoptosis and necrosis in cells. This study developed a biochip system for inexpensive, simple, and capable of distinguishing between live, apoptotic, and necrotic cells. This biochip system (70 x 150 x 80 mm) comprises a slide into which fluorescently stained cells are injected, an LED light source, and a camera system. When cells stained with a fluorescent reagent are irradiated at the excitation wavelength, they fluoresce. By changing the combination of fluorescent reagent and excitation wavelength, live, apoptotic, and necrotic cells can be photographed. Then they are processed by a cell counting program using existing methods to determine numbers of live, apoptotic, and necrotic cells. To demonstrate the effectiveness of this system, we conducted live cell, apoptosis, and necrosis detection experiments using colon cancer cells. Results of each experiment using the biochip system were compared with visual cell counts made by an operator. The novel biochip system successfully distinguishes between live, apoptotic and necrotic cells. Detection time was <1 s, and the detection error was 9%, compared to visual inspection. The system in this study could reduce the cost and time of tasks requiring cell observation, such as biological detection and disease diagnosis, as well as provide a convenient method for testing the effectiveness of deeper approaches.

INDEX TERMS Biochip, Cell observation, Image Processing

I. INTRODUCTION

Cell culture is fundamental for basic research and regenerative medicine[1], [2], [3], and cell observation is one of the essential tasks in cell culture[4], [5], [6], [7]. Cell counting is of great use in biological detection and diagnosis of disease. For example, it can be used to determine the amount of reagents and chemicals used in experiments, in cancer treatment and in the early detection of disease[8], [9], [10], [11], [12], [13]. During cell culture, status of individual cells is observed by an operator using a light microscope; however, analysis of cultured cells can be performed automatically using a dedicated cell analysis instrument[7].

Microscopy allows an operator to evaluate cells intuitively, but is not suitable for examining large quantities of cells, and has the disadvantage of inter-operator differences in evaluation and it is extremely time-consuming[7], [14], [15], [16].

On the other hand, instrumental cell observation allows objective evaluation by software more quickly than by a human operator, but dedicated instruments have the disadvantage of being expensive to install and maintain[17], [18]. Flow cytometers (fluorescence-activated cell sorting, hereafter FACS) and cell counters are the primary devices used for cell analysis. The cell counter is smaller and less expensive than other cell analysis devices such as flow cytometers (FACS) and real-time PCR (about $13,000), and requires less start-up and shutdown time. Cell counters can determine whether fluorescently stained cells are alive or dead. Cell death can be roughly divided into two types: apoptosis and necrosis, but Cell counters cannot distinguish

apoptosis from necrosis in dead cells[19], [20], [21], [22]. Distinguishing between apoptosis and necrosis is very important in determining whether an approach to cells is effective. This is because the number of apoptotic cells, or the ratio of apoptosis to necrosis, is often used to describe the efficacy of a new approach to cancer treatment[23],[24], [25], [26], [27].

To overcome these problems, we developed a biochip system to achieve inexpensive, simple, and capable of distinguishing between live, apoptotic and necrotic cells. This system consists of a slide into which stained cells are injected, an LED light source, and an optical system, including a CCD camera. Stained cells are irradiated at an excitation wavelength, and resulting fluorescence images are processed to determine cell states.

This paper describes the configuration of the biochip system, and explains the fluorescent cell counting program. Finally, experiments were conducted to demonstrate the system's effectiveness in detecting live cells, apoptotic cells and necrotic cells using colon cancer cells. Each experiment compared the number of cells detected and the time required for detection between cell counting using the biochip system and visual cell counting by an operator. The results obtained indicate that the system in this study can reduce the cost and time of tasks requiring cell observation, as well as provide a convenient method for testing the effectiveness of deeper approaches. Even researchers without large budgets can fabricate this system to at least discriminate between live, apoptotic, and necrotic cells without spending a lot of money. Reproducing the system would also be relatively easy since a 3D printer is used to fabricate the parts. The system also allows for easy cell counting by both the public and experts.

II. MATERIALS AND METHOD

A. BIOCHIP CELL ANALYSIS SYSTEM

1) SYSTEM CONFIGURATION

Theconfiguration of the biochip system for cell analysis is shown in FIGURE 1. Cells stained with fluorescent reagents are injected into a slide, and LEDs of wavelengths appropriate for these fluorescent reagents are used to irradiate the cells. A controller enables adjustment of LED irradiation type and intensity. LED light excites the fluorescent reagent, causing the cells to fluoresce. A bandpass filter for fluorescence separates the mixture of LED light and cell fluorescence, allowing only emitted fluorescence to pass through. A CCD camera then captures the fluorescence, and a cell counting program analyzes the resulting images. In this study, the following fluorescent reagents were used to observe different cell characteristics: Calcein Blue (AAT Bioquest, USA) for live cells, Annexin V-FITC (Medical & Biological Laboratories, Japan) for apoptotic cells, and propidium iodide (PI: Medical & Biological Laboratories, Japan) for necrotic cells. Staining targets, excitation wavelengths, and fluorescence wavelengths of these reagents are listed in Table 1[28], [29], [30].

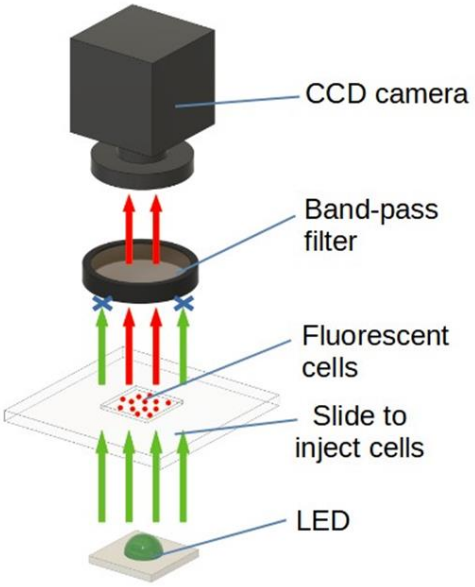

FIGURE 1. System configuration

TABLE 1
Characteristics of fluorescent reagents

Name	Staining target	Excitation λ	Emission λ
Calcein Blue	Live cells	354nm	441nm
Annexin V-FITC	Apoptotic cells	494nm	518nm
PI	Necrotic cells	530nm	620nm

This system used OSV1XME3E1S (peak wavelength 365 nm, OpyoSupply, Hong Kong), GC VJLPE1.13 (peak wavelength 490 nm, OSRAM, Germany) and LXML-PM01-0100 (peak wavelength 530 nm, Lumileds, USA) LEDs, respectively, to excite Calcein Blue, Annexin V-FITC and PI. Three fluorescence bandpass filters with center wavelengths of 440 nm, 525 nm, and 620 nm (#86-350, #86-984, #33-910, Edmund Optics, USA) were employed for fluorescence separation. The CCD camera utilized in this system was a 3R-MSUSB501 (3R Solution, Japan).

2) FABRICATED BIOCHIP

The biochip system and its structure are shown in FIGURES 2 and FIGURE 3. A 3D printer (Anycubic Mega X, Anycubic, USA) was utilized to fabricate several components of the device, including the base, LED stand, slide stand, fluorescent bandpass filter stand and CCD camera stand. Device dimensions are approximately 70 mm x 150 mm x 80 mm (L x W x H). Three LEDs are mounted on the LED stand with appropriate heat sinks for heat dissipation. In this case, GC VJLPE1.13 and LXML-PM01-0100 were mounted on a single heat sink. LEDs can be switched by sliding the LED stand while maintaining a consistent height. The narrowest field of view (half angle) of the LEDs is 120°. Accordingly, the slide stand is placed at a height such that LED light illuminates the entire cell. This study used commercially available cell counter slides (LUNA Cell Counting Slides,

Logos biosystems, Korea) for cell injection. A slide is fixed to the slide stand and cannot be moved during cell observation. The CCD camera stand is positioned at a height such that the focus is at the position of the slide when the CCD camera is set to approximately 200 × magnification. This condition reduces the time required for focusing the camera when observing cells.

FIGURE 2. **Biochip system**

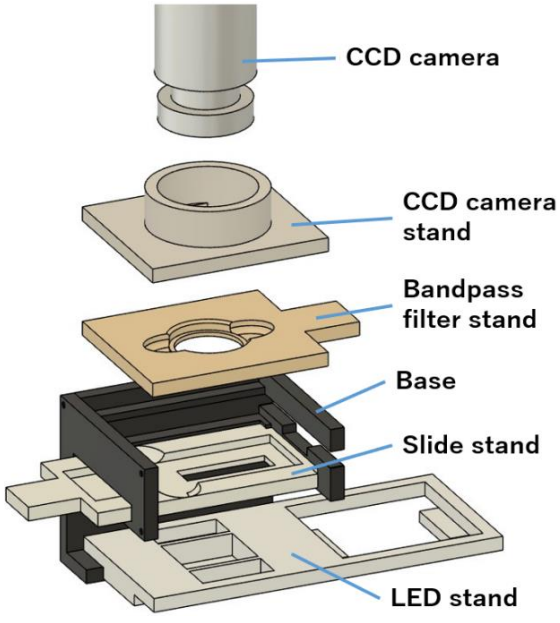

FIGURE 3. **System structure**

B. CELL COUNTING PROGRAM

To count cells in fluorescent images obtained using the biochip system, a simple cell counting program was created using conventional methods. The development environment for the cell counting program is shown in TABLE 2.

TABLE 2
Development environment for cell counting program

OS	Windows 10 Home 22H2
Library	OpenCV 1.78.0 (user setup)
Language	Python 3.9.0

The following is an overview of the cell counting program:

1. Binarizes fluorescence images of cells captured by a CCD camera.
2. Generates a distance map based on Binarized images.
3. Identifies the pixel with the highest value in the surrounding area and determines the number of cells.

A distance map described in step 2 is an image in which the value of each pixel is replaced by the distance to the nearest pixel with a value of 0[31]. The distance map is used to identify neighboring objects individually. It enables accurate cell counting, even in areas where cells partially overlap. However, when a distance map is created, a given pixel may have the same value as a nearby pixel. In this case, detecting the pixel with the largest value among surrounding pixels in step 3 might detect a single cell as multiple cells. To address this problem, expansion processing is applied before counting cells. This process makes it possible to count maximum value pixels as single cells when they are close to each other. The distance map was created using the cv2.distanceTransform function provided by OpenCV, and the mask size was set to 5. The kernel for the magnification process was a rectangle of size 3 x 3. This is because, due to the size of the image used in this study, cells can be considered as one if the kernel size is larger than 3 x 3. This method is a classic cell counting technique. We chose this method because it was easy to implement.

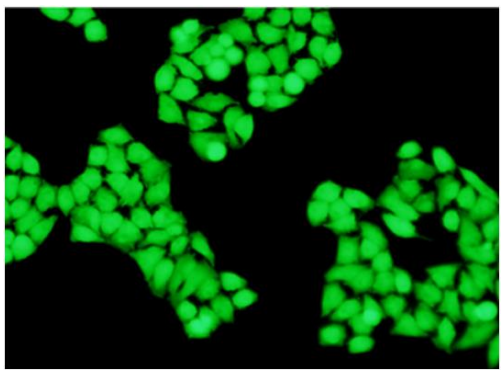

FIGURE 4. **Cells stained with calcein-AM (x400)**

C. EXPERIMENTS

1) TRIAL CELL COUNTING PROGRAM

Images of fluorescently stained cells were used to validate the cell counting program. FIGURE 4 and FIGURE 5 show sample images. FIGURES 4 and FIGURE 5 are images of fluorescently stained cells (published by Dojin Chemical Laboratory, Japan) [28]. FIGURE 4 shows an image of cultured HeLa cells stained with calcein-AM and irradiated at the excitation wavelength. FIGURE 5 shows a picture of

cultured cells stained with PI and irradiated at the excitation wavelength.

Calcein-AM is a fluorescent reagent commonly used to observe living cells. Its excitation and emission wavelengths are 496 nm and 520 nm [32]. We ran the program against FIGURES 4 and FIGURE 5 to count cells. Visual counts were also performed.

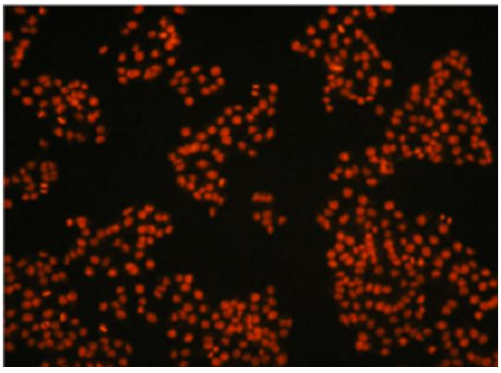

FIGURE 5. Cells stained with PI (x200)

2) BIOCHIP SYSTEM PERFORMANCE EVALUATION EXPERIMENTS

Experiments were conducted to assess the performance of the novel biochip system. Using cultured colon carcinoma cells (CW-2, RCB0778, RIKEN BioResource Research Center, Japan), we confirmed that using fluorescence, the system can distinguish apoptotic and necrotic cells. The experimental procedure is shown below:

1. Cultured colon cancer cells were irradiated with UV light to induce apoptosis/necrosis and double-stained with Annexin V-FITC and PI[33], [34], [35].
2. 10 μL of stained colon cancer cells were injected into a slide, observed, and photographed. Cell fluorescence was observed and photographed when two wavelengths of excitation light were used with the biochip system.

In Step 1, colon cancer cells were initially incubated at 37° C in a 5% CO_2 environment for 72 h using RPMI-1640 (189-02025, FUJIFILM Wako Pure Chemical Corporation, Japan, stock solution)＋FBS10% medium (FBS South America, S1810-500, BioWest, France) (cell density 1×106 cells/ml). Subsequently, cells were irradiated with 365 nm light at a dose of 60 J/cm^2 ;33.3 sec. Following UV exposure, cells were incubated another 48 h at 37°C in 5% CO_2. In Step 2, cellular fluorescence was observed and captured when irradiated at 490 nm (image resolution 96 dpi). Afterward, fluorescence was observed and captured when cells were irradiated at 530 nm (image resolution 96 dpi). The two fluorescent images obtained in this way were compared to confirm that the developed biochip system could distinguish and identify cells that fluoresced with different fluorescent reagents.

3) CELL DETECTION EXPERIMENTS

Cell detection experiments were conducted using the new biochip system and the cell counting program was employed to detect live, apoptotic and necrotic cells among cultured colon carcinoma cells (CW-2, RCB0778, RIKEN BioResource Research Center, Japan). Accuracy of the analysis was assessed by comparing cell counts obtained from the program with those obtained through visual counting. The experiment was performed as follows:

1. Cultured colon cancer cells were irradiated with UV light to induce apoptosis/necrosis and stained with Annexin V-FITC and PI.
2. Cultured colon cancer cells were stained with Calcein Blue.
3. 10 μL of stained colon cancer cells were injected into a slide, and their fluorescence was observed and photographed using the biochip system.
4. Four 1 x 1 mm areas were cropped from each of the Calcein blue fluorescent images, the Annexin V-FITC fluorescent images, and the PI fluorescent images obtained in step 3. The cell counting program was executed for each image to count numbers of cells and to record the time to complete the count.
5. Visual counting of cells was performed for the image in step 4, and the time required to complete the count was measured.
6. Numbers of cells and the time taken to count the cells were compared between the cell counting program and visual counting.

In Step 1, colon cancer cells were initially incubated at 37°C in a 5% CO_2 environment for 72 h. The culture medium conditions and cell density were the same as in the biochip system performance evaluation experiments. Subsequently, cells were divided into those irradiated with 365 nm light at a dose of 30 J/cm^2 ;16.7 min (inducing apoptosis) and those irradiated with 100 J/cm^2 ;55.6 min (inducing necrosis), and these cells were incubated for another 48 h at 37°C in 5% CO_2. In Step 2, after colon cancer cells were incubated for 72 h at 37°C in a 5% CO2 environment, they were transferred to Petri dishes and incubated for another 48 h. These are used as controls (live cells). In Step 3, three slides each injected with live, apoptosis and necrosis cells were prepared, and 9 images were taken of each slide (image resolution 96 dpi). For step 5, to minimize evaluation bias due to individual differences, several operators performed visual cell counting, and the average of the results was treated as the result of visual cell counting. Five operators who understood how to count cells were involved in this experiment. All operators counted cells without knowing the results of the cell counting program or counts of other operators.

III. RESULT

A. RESULTS OF PROGRAM TRIALS

We ran the program against FIGURES 4 and FIGURE 5 to count cells. Visual counts were also performed. In Figure 6, yellow dots mark the coordinates of detected cells shown in FIGURE 5. Vertical and horizontal axes of FIGURE 6 represent numbers of pixels. FIGURE 7 shows partially magnified versions of FIGURES 5 and FIGURE 6 to confirm the results. Blue circles in FIGURE 7 emphasize areas in which comparisons are most apparent. FIGURE 7 shows that yellow dots are drawn separately, even in areas where cells are rather dense, confirming that these cells can be detected individually. Visual counts are performed for FIGURE 4 and FIGURE 5. Results of the program and visual counts are shown in TABLE 3.

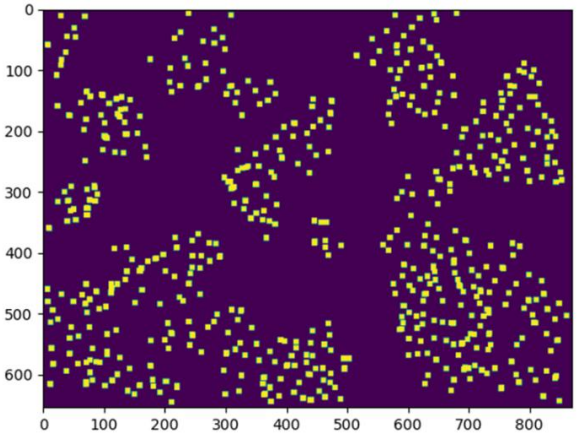

FIGURE 6. Program execution example

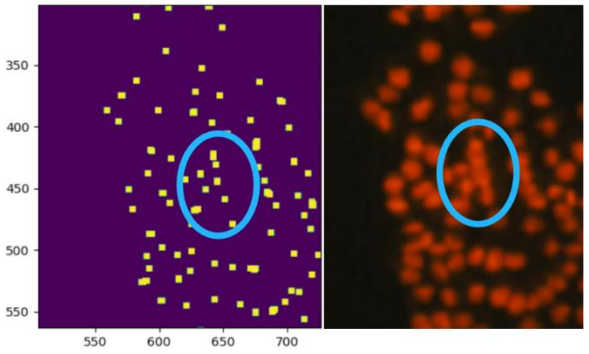

FIGURE 7. Checking the results of the program execution

TABLE 3
Results of program trials

	Calcein-AM	PI
Program	117 cells	552 cells
Operator	130 cells	568 cells

B. RESULTS OF BIOCHIP SYSTEM PERFORMANCE EVALUATION EXPERIMENTS

Experiments were conducted to assess the performance of the novel biochip system. FIGURES 8 shows Annexin V-FITC excited at 490 nm, and FIGURES 9 shows the same field when excited at 530 nm. FIGURES 8 and FIGURES 9 show images taken without moving the slide or the CCD camera, but there was a slight rotation. This shift was due to the gap between the CCD camera stand and the base of the biochip system. To compare fluorescence, the areas surrounded by orange squares in FIGURES 8 and FIGURES 9 were enlarged and aligned in FIGURES 10.

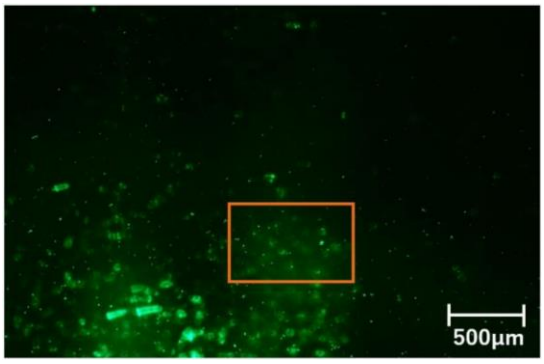

FIGURE 8. Fluorescence of gastric cancer cells stained with An-nexin V-FITC (×200)

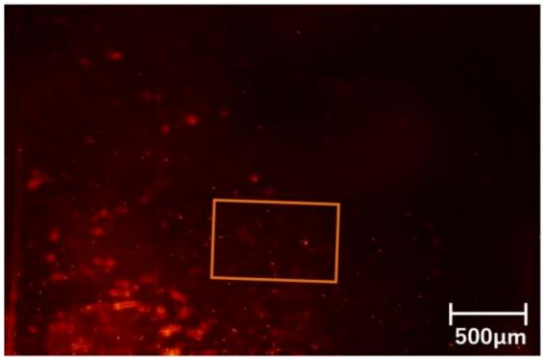

FIGURE 9. Fluorescence of gastric cancer cells stained with PI (×200)

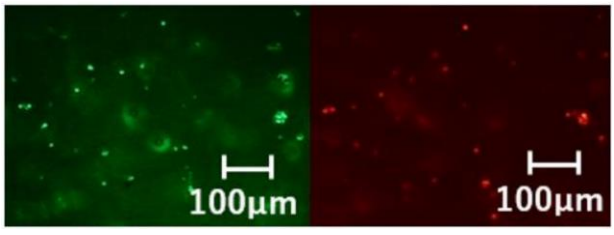

FIGURE 10. Comparison of fluorescence

FIGURES 10 demonstrates variation in numbers and spatial distribution of fluorescing cells in the same group. This observation demonstrates that the biochip system can distinguish and identify cells that fluoresced with different fluorescent reagents.

C. RESULTS OF CELL DETECTION EXPERIMENT

Numbers of live, apoptotic and necrotic cultured colon cancer cells were counted using the biochip system. FIGURES 11 shows fluorescence of Calcein Blue excited by an LED at 365 nm, FIGURES 12 shows fluorescence of Annexin V-FITC excited by an LED at 490 nm, and FIGURES 13 shows

fluorescence of PI excited by an LED at 530 nm. Four 1 × 1 mm sections were cut from each image in FIGURES 11, FIGURES 12 and FIGURES 13 and used as images for cell counting. An example is shown in FIGURES 14.

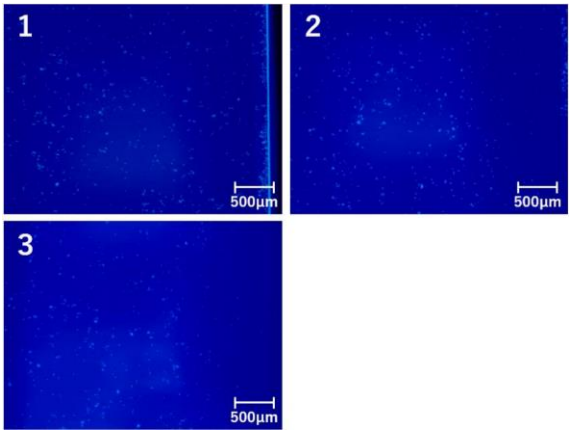

FIGURE 11. **Fluorescence of gastric cancer cells stained with Calcein Blue (×200)**

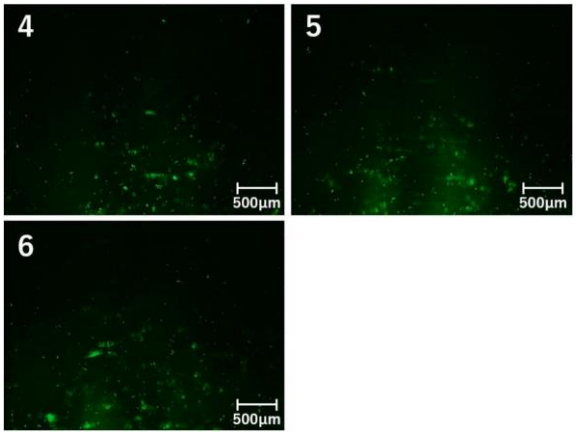

FIGURE 12. **Fluorescence of gastric cancer cells stained with Annexin V-FITC after induction of apoptosis (×200)**

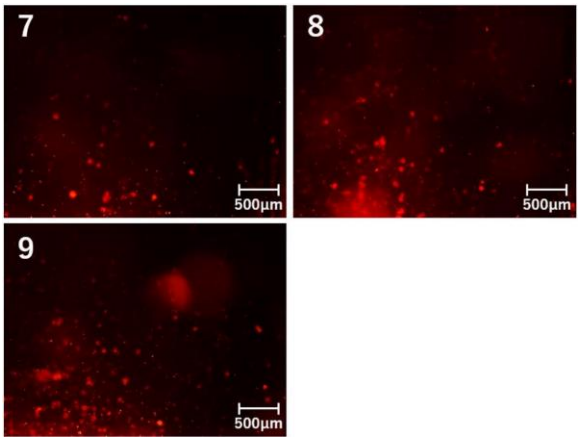

FIGURE 13. **Fluorescence of gastric cancer cells stained with Annexin PI after induction of necrosis (×200)**

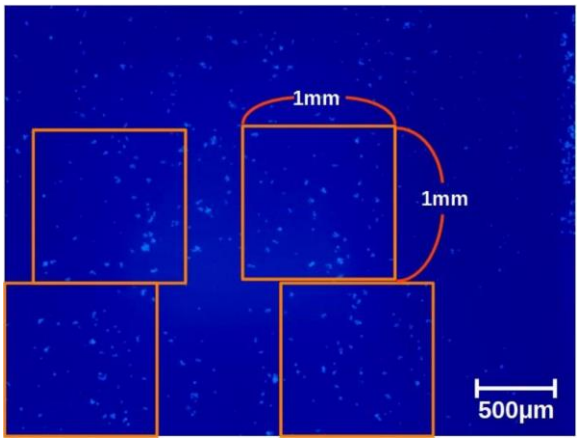

FIGURE 14. **Cut four 1 x 1 mm sections from one image**

The developed cell counting program was executed on the 36 images obtained. Concurrently, operators performed the counts. Results for each image in FIGURES 11 are shown in TABLE 4. Results for each image in FIGURES 12 are shown in TABLE 5, and results for each image in FIGURES 13 are shown in TABLE 6. The average number of detected cells is the average count of cells in the image for the four images cut from each image in FIGURES 11-14. The average detection time is the average time the cell counting program or an operator took to count cells for each image and to determine that all cells had been counted (TABLES 4-6).

TABLE 4
Cell counts for calcein blue images

Operator	Average Numbers of detected cells			Average detection time [s]
	1	2	3	
A	73	68	52	53.3
B	67	58	53	55
C	66	71	58	53.3
D	63	58	42	73.7
E	70	63	48	59.7
Visual average	68	64	51	59
Program	73	67	52	0.64

TABLE 5
Cells counts for Annexin V-FITC images

Operator	Average Numbers of detected cells			Average detection time [s]
	4	5	6	
A	50	49	37	38.3
B	52	53	39	42.7
C	54	51	37	40.3
D	55	50	38	44.7
E	55	50	35	41.3
Visual average	53	51	37	53.8
Program	52	50	34	0.63

TABLE 6
Cells counts for PI images

Operator	Average Numbers of detected cells			Average detection time [s]
	7	8	9	
A	26	20	37	23.3
B	29	22	44	28.7
C	33	26	46	36.3
D	27	23	42	31.7
E	26	18	35	23.3
Visual average	28	22	41	46.9
Program	26	21	40	0.64

IV. DISCUSSION

TABLE 3 demonstrates that the cell counting program detects as many cells as visual counting. Differences in numbers of cells detected by visual and programmed counts could be due to the fact that binarized images and distance maps were not properly created because there were areas in which cells were so close together that there was little difference in luminance. In addition, some cells located at the edges of the sample image may not have been visible, and as a result, could not be counted. It is also possible that operators miscounted some cells visually.

Two-tailed t-tests were performed for TABLE 4 to TABLE 6 at a 5% dominance level between the visual average and the program. The results were p=0.12169 for TABLE 4, p=0.129612 for TABLE 5, and p=0.057191 for TABLE 6, all greater than 0.05. This means that there was no significant difference between the average of the visual cell counts and the cell counts performed by the program.

In TABLE 4 to TABLE 6, when presented as the ratio of the number of cells detected by the program divided by those detected visually, FIGURE 6 (TABLE 5) had the worst result, at 8.1%. This result may be due to the small number of cells in the image, as well as both bright and dark areas in the image, which made it difficult for the program to count cells.

Comparing the number of cells detected by the program to the visual average, the largest difference was seen in image 1, with a discrepancy of 5 cells (7.4%). One possible reason for the higher number of cells detected by the program could be that there were several areas where cells were dense and difficult for the operators to count. Thus, the actual biochip error is likely to be significantly smaller than 9%.

These results indicate that the novel biochip system and cell counting program complete analysis with a detection time <1 s and nearly the same accuracy as visual counting; thus, this biochip system can reduce the time and cost of cell analysis. This system is also superior in terms of cost. While a typical cell counter costs about $13,000 and a FACS costs more than $67,000 for the main unit alone, the cost of this system was about $1,200.

V. CONCLUSION

This study developed a fast and simple biochip system and cell counting program to discriminate between live cells and apoptotic and necrotic cells, which Cell counters are unable to do. After evaluating the system, experiments were conducted to detect live, apoptotic and necrotic cells among cultured colon cancer cells using the biochip system and cell counting program. As a result, the novel biochip system distinguished between live, apoptotic and necrotic cells. The system also achieved nearly the same accuracy of analysis as visual counting, with a detection time <1 s and at a lower cost. Kang et al. are developing a smartphone-based cell counter to determine whether cells are alive or dead. In contrast, to our knowledge, the system in this study is the first system that can distinguish between live, apoptotic, and necrotic cells at such a low cost[21]. These results indicate that this system has the potential to reduce the cost and time of tasks requiring cell observation, as well as provide a convenient method for testing the effectiveness of deeper approaches. For example, the system could be used to determine the percentage of apoptotic cells in a drug screening or to observe cells in a disease diagnosis, allowing more detailed analysis than cell counters without the time-consuming FACS. Even researchers without a large budget can fabricate this system to at least distinguish between live, apoptotic, and necrotic cells without spending a lot of money. An inexpensive FDM 3D printer is used to fabricate the parts of this system. Since 3D printers are becoming increasingly popular these days, it will be relatively easy to reproduce the system if we publish 3D CAD data in the future. The system also allows for easy cell counting by both the public and experts.

However, there are many aspects of this system that need improvement. Power LEDs were used because the irradiation intensity required to excite the fluorescent reagents used was unknown, but irradiation intensity exceeding that required can damage cells and interfere with fluorescence imaging. From the standpoint of reproducibility and suitability, the choice of light sources and fluorescent reagents can be controversial. Although the device itself does not require a large space for installation, it cannot be installed anywhere and is not freely portable because it requires power from an electrical outlet. Consideration of the accuracy and robustness of the program and comparison with other methods will also be an issue for the future.

In the future, comparative experiments will be conducted using a commercially available cell counter, as well as to miniaturize the biochip system to a size that is portable.

ACKNOWLEDGMENT

We did not receive any grants for this study from any funding entity in the public, commercial, or non-profit sectors.

REFERENCES

[1] R. I. Freshney, Culture of Animal Cells: A Manual of Basic Technique and Specialized Applications. John Wiley & Sons, 2015.
[2] S. Fagète, C. Steimer, and P.-A. Girod, “Comparing two automated high throughput viable-cell counting systems for cell culture applications,” J. Biotechnol., vol. 305, pp. 23–26, Nov. 2019, doi: 10.1016/j.jbiotec.2019.08.014.

[3] A. Vembadi, A. Menachery, and M. A. Qasaimeh, "Cell Cytometry: Review and Perspective on Biotechnological Advances," Front. Bioeng. Biotechnol., vol. 7, 2019, Accessed: Oct. 25, 2023. [Online]. Available: https://www.frontiersin.org/articles/10.3389/fbioe.2019.00147
[4] D. Cadena-Herrera et al., "Validation of three viable-cell counting methods: Manual, semi-automated, and automated," Biotechnol. Rep., vol. 7, pp. 9–16, Sep. 2015, doi: 10.1016/j.btre.2015.04.004.
[5] R. Green and S. Wachsmann-Hogiu, "Development, History, and Future of Automated Cell Counters," Clin. Lab. Med., vol. 35, no. 1, pp. 1–10, Mar. 2015, doi: 10.1016/j.cll.2014.11.003.
[6] P. Manzini, V. Peli, A. Rivera-Ordaz, S. Budelli, M. Barilani, and L. Lazzari, "Validation of an automated cell counting method for cGMP manufacturing of human induced pluripotent stem cells," Biotechnol. Rep., vol. 33, p. e00708, Mar. 2022, doi: 10.1016/j.btre.2022.e00708.
[7] J. S. Kim et al., "Comparison of the automated fluorescence microscopic viability test with the conventional and flow cytometry methods," J. Clin. Lab. Anal., vol. 25, no. 2, pp. 90–94, 2011, doi: 10.1002/jcla.20438.
[8] C. A. Bravery and A. French, "Reference materials for cellular therapeutics," Cytotherapy, vol. 16, no. 9, pp. 1187–1196, Sep. 2014, doi: 10.1016/j.jcyt.2014.05.024.
[9] K. Domińska, A. W. Piastowska-Ciesielska, A. Lachowicz-Ochędalska, and T. Ochędalski, "Similarities and differences between effects of angiotensin III and angiotensin II on human prostate cancer cell migration and proliferation," Peptides, vol. 37, no. 2, pp. 200–206, Oct. 2012, doi: 10.1016/j.peptides.2012.07.022.
[10] E. O'Neil, S. Burton, B. Horney, and A. MacKenzie, "Comparison of white and red blood cell estimates in urine sediment with hemocytometer and automated counts in dogs and cats," Vet. Clin. Pathol., vol. 42, no. 1, pp. 78–84, 2013, doi: 10.1111/vcp.12004.
[11] S. Ito, Y. Fujino, S. Ogata, M. Hirayama-Kurogi, and S. Ohtsuki, "Involvement of an Orphan Transporter, SLC22A18, in Cell Growth and Drug Resistance of Human Breast Cancer MCF7 Cells," J. Pharm. Sci., vol. 107, no. 12, pp. 3163–3170, Dec. 2018, doi: 10.1016/j.xphs.2018.08.011.
[12] M. T. May et al., "Impact on life expectancy of HIV-1 positive individuals of CD4+ cell count and viral load response to antiretroviral therapy," AIDS Lond. Engl., vol. 28, no. 8, pp. 1193–1202, May 2014, doi: 10.1097/QAD.0000000000000243.
[13] B. J. McMullan, D. Desmarini, J. T. Djordjevic, S. C.-A. Chen, M. Roper, and T. C. Sorrell, "Rapid Microscopy and Use of Vital Dyes: Potential to Determine Viability of Cryptococcus neoformans in the Clinical Laboratory," PLoS ONE, vol. 10, no. 1, p. e0117186, Jan. 2015, doi: 10.1371/journal.pone.0117186.
[14] Goda K. et al., "High-throughput single-microparticle imaging flow analyzer," Proc. Natl. Acad. Sci., vol. 109, no. 29, pp. 11630–11635, Jul. 2012, doi: 10.1073/pnas.1204718109.
[15] D. B. DeNicola, "Advances in Hematology Analyzers," Top. Companion Anim. Med., vol. 26, no. 2, pp. 52–61, May 2011, doi: 10.1053/j.tcam.2011.02.001.
[16] S. S. Alahmari, D. Goldgof, L. Hall, H. A. Phoulady, R. H. Patel, and P. R. Mouton, "Automated Cell Counts on Tissue Sections by Deep Learning and Unbiased Stereology," J. Chem. Neuroanat., vol. 96, pp. 94–101, Mar. 2019, doi: 10.1016/j.jchemneu.2018.12.010.
[17] E. van der Pol et al., "Particle size distribution of exosomes and microvesicles determined by transmission electron microscopy, flow cytometry, nanoparticle tracking analysis, and resistive pulse sensing," J. Thromb. Haemost., vol. 12, no. 7, pp. 1182–1192, Jul. 2014, doi: 10.1111/jth.12602.
[18] M. Gunetti et al., "Validation of analytical methods in GMP: The disposable Fast Read 102® device, an alternative practical approach for cell counting," J. Transl. Med., vol. 10, no. 1, 2012, doi: 10.1186/1479-5876-10-112.
[19] K. H. Jones and J. A. Senft, "An improved method to determine cell viability by simultaneous staining with fluorescein diacetate-propidium iodide.," J. Histochem. Cytochem., vol. 33, no. 1, pp. 77–79, Jan. 1985, doi: 10.1177/33.1.2578146.
[20] M. Fricker, A. M. Tolkovsky, V. Borutaite, M. Coleman, and G. C. Brown, "Neuronal Cell Death," Physiol. Rev., vol. 98, no. 2, pp. 813–880, Apr. 2018, doi: 10.1152/physrev.00011.2017.
[21] W. Kang et al., "On-site cell concentration and viability detections using smartphone based field-portable cell counter," Anal. Chim. Acta, vol. 1077, pp. 216–224, Oct. 2019, doi: 10.1016/j.aca.2019.05.029.
[22] B. Kim, Y. J. Lee, J. G. Park, D. Yoo, Y. K. Hahn, and S. Choi, "A portable somatic cell counter based on a multi-functional counting chamber and a miniaturized fluorescence microscope," Talanta, vol. 170, pp. 238–243, Aug. 2017, doi: 10.1016/j.talanta.2017.04.014.
[23] L. Bai et al., "47kDa isoform of Annexin A7 affecting the apoptosis of mouse hepatocarcinoma cells line," Biomed. Pharmacother., vol. 83, pp. 1127–1131, Oct. 2016, doi: 10.1016/j.biopha.2016.08.007.
[24] E. Koç, S. Çelik-Uzuner, U. Uzuner, and R. Çakmak, "The Detailed Comparison of Cell Death Detected by Annexin V-PI Counterstain Using Fluorescence Microscope, Flow Cytometry and Automated Cell Counter in Mammalian and Microalgae Cells," J. Fluoresc., vol. 28, no. 6, pp. 1393–1404, Nov. 2018, doi: 10.1007/s10895-018-2306-4.
[25] L. C. Crowley, B. J. Marfell, A. P. Scott, and N. J. Waterhouse, "Quantitation of Apoptosis and Necrosis by Annexin V Binding, Propidium Iodide Uptake, and Flow Cytometry".
[26] T. El-Sewedy et al., "Hepatocellular Carcinoma cells: activity of Amygdalin and Sorafenib in Targeting AMPK /mTOR and BCL-2 for anti-angiogenesis and apoptosis cell death," BMC Complement. Med. Ther., vol. 23, no. 1, p. 329, Sep. 2023, doi: 10.1186/s12906-023-04142-1.
[27] M. E. Guicciardi, H. Malhi, J. L. Mott, and G. J. Gores, "Apoptosis and Necrosis in the Liver," Compr. Physiol., vol. 3, no. 2, p. 10.1002/cphy.c120020, Apr. 2013, doi: 10.1002/cphy.c120020.
[28] "catalog-project.pdf." Accessed: Nov. 02, 2023. [Online]. Available: https://www.dojindo.co.jp/technical/pdf/catalog-project.pdf
[29] "TFS-AssetsLSGmanualsmp13199.pdf." Accessed: Nov. 02, 2023. [Online]. Available: https://assets.thermofisher.com/TFS-Assets%2FLSG%2Fmanuals%2Fmp13199.pdf
[30] "protocol-for-calcein-blue-am-cas-168482-84-6-version-45997d0d78.pdf." Accessed: Nov. 02, 2023. [Online]. Available: https://docs.aatbio.com/products/protocol-and-product-information-sheet-pis/protocol-for-calcein-blue-am-cas-168482-84-6-version-45997d0d78.pdf
[31] G. Borgefors, "Distance transformations in digital images," Comput. Vis. Graph. Image Process., vol. 34, no. 3, pp. 344–371, Jun. 1986, doi: 10.1016/S0734-189X(86)80047-0.
[32] Xiu Ming Wang, P. I. Terasaki, G. W. Rankin, D. Chia, Hui Ping Zhong, and S. Hardy, "A new microcellular cytotoxicity test based on calcein AM release," Hum. Immunol., vol. 37, no. 4, pp. 264–270, Aug. 1993, doi: 10.1016/0198-8859(93)90510-8.
[33] S. Inada et al., "Development of an Ultraviolet A1 Light Emitting Diode-based Device for Phototherapy," Oct. 2023.
[34] S. A. Inada, "Investigation of Effective UVA1 Peak Wavelength Range to Application on Phototherapy," vol. 5, no. 2, 2018.
[35] S. A. Inada, "The New Method for Bacterial Sterilization by Using UVA1 Range Light Emitting Diode," vol. 6, no. 1, 2019.

AUTHOR BIOGRAPHY

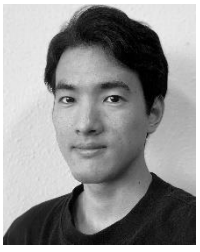

Masato Sawatari was born in 1999 in Kumamoto, Japan. He received the B.S. degree in Faculty of Engineering from Kumamoto University, Kumamoto, Japan, in 2022. Since 2022, He has been a student with the Graduate School of Science and Technology, Kumamoto University, Kumamoto, Japan. His research interests include biomedical engineering, especially optical devices for the treatment of cancer.

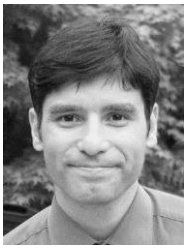

Shunko A. Inada was born in Cordoba, Argentina in 1980. He received the B.S. degree in electrical and electronic engineering in 2003, and the M. S. degree in material engineering in 2006, and Ph. D. degree in electrical and electronic engineering from Meijo University, Nagoya, Japan, in 2012. From 2012 to 2015, he was a postdoctoral researcher with the Graduate School of Engineering, Nagoya University, Aichi, Japan. From 2015 to 2020, he was an assistant professor with the Graduate School of Engineering, Hirosaki University, Aomori, Japan. Since 2020, he has been an assistant professor with the Faculty of Advanced Science and Technology, Kumamoto University, Kumamoto, Japan. He works on the research of biomedical engineering especially for treatment of skin disease and cancer.